Single-Turnover Analysis of Mutant Human Apurinic/Apyrimidinic Endonuclease[†,‡]

Julie A. Lucas,[§] Yuji Masuda,[||,⊥] Richard A. O. Bennett,[||] Nathaniel S. Strauss,[§,@] and Phyllis R. Strauss*[,§]

Department of Biology, Northeastern University, Boston, Massachusetts 02115, Department of Cancer Cell Biology, Harvard School of Public Health, Boston, Massachusetts 02115, and Department of Chemistry, The Pennsylvania State University, University Park, Pennsylvania 16802

Received August 25, 1998; Revised Manuscript Received February 8, 1999

ABSTRACT: Apurinic/apyrimidinic endonuclease (AP endo) is a key enzyme in the repair of oxidatively damaged DNA. Using single-turnover conditions, we recently described substrate binding parameters for wild type human AP endo. In this study, we utilized four enzyme mutants, D283A, D308A, D283A/D308A, and H309N, and assayed them under steady state and single-turnover conditions. The turnover number of the single aspartate mutants was decreased 10−30-fold in comparison to that of the wild type. The decrease in the turnover number was accompanied by a 17- and 50-fold decrease in the forward rate constant (k_{on}) for substrate binding by D308A and D283A, respectively. The dissociation rate constant for substrate (k_{off}) was unchanged for the D308A mutant but was 10 times faster for the D283A mutant than for the wild type. The apparent K_m values for both of the single aspartate mutants were about equal to their respective K_D values. To account for the kinetic behavior of the D308A mutant, it was necessary to insert a conformational change into the kinetic scheme. In contrast to the single aspartate mutants, the turnover number for the double mutant was 500-fold lower than that of the wild type, its apparent K_m was 2.5-fold higher, and binding to substrate was weak. Mutation of His^{309} caused the greatest decrease in activity, resulting in a turnover number that was more than 30000-fold lower than that of the wild type and an apparent K_m that was 13-fold higher, supporting the notion that His^{309} is intimately involved in catalysis. Molecular dynamics simulation techniques suggested that conversion of either aspartate to alanine resulted in major shifts in the spatial localization of key amino acids. Despite the fact that the two aspartates flank His^{309}, the movement they engendered was distinct, consistent with the differences in catalytic behavior. We suggest that the conformation of the active site is largely maintained by the two aspartates, which enable efficient binding and cleavage of abasic site-containing DNA.

Apurinic/apyrimidinic endonuclease (AP endo) is a human enzyme that is critical to the repair of abasic sites in DNA arising through either base excision repair or oxidative damage. AP endo recognizes abasic sites in DNA and cleaves the phosphodiester backbone 5′ to the abasic site. Both steady state (*1*−*3*) and single-turnover (*1*) kinetic assays have been performed on wild type AP endo, demonstrating a Briggs−Haldane mechanism. In the absence of physical methods for observing catalysis directly during millisecond intervals, single-turnover measurements make it possible to observe a single catalytic event. The single-turnover assays were possible because of the discovery of an extremely efficient inhibitor of AP endo. This inhibitor, known as HDP, is the β-elimination product of an abasic site which forms during heating.

The three-dimensional structure of human AP endo has been determined by X-ray crystallography (*4*). Some of the polar residues that are present at the proposed active site of AP endo are Glu^{96}, Asp^{283}, Asp^{308}, and His^{309} (*4*−*8*). The Glu^{96} residue is believed to bind the metal cation required for catalysis, while the other residues are thought to be required for substrate binding and cleavage of the DNA backbone. To test this hypothesis, we utilized four enzyme mutants, D283A, D308A, D283A/D308A, and H309N, to measure both steady state and substrate binding parameters. In the case of the first three mutants, alanine was substituted for aspartate to remove a negative charge that might be involved in the orientation of active site residues or aligning either the divalent cation or the substrate or both; in the case of the H309N mutant, we replaced a basic amino acid containing an aromatic ring with the amide of an acidic amino acid that retained the relative position of the nitrogen at position 4 but removed the potential for a positive charge at position 2 and subsequent resonance structures.

In addition to the kinetic studies, we have also simulated the structural changes that mutation of the key residues might confer. Comparisons of the kinetic constants of the mutants to those of native AP endo and the simulated structural changes provide us with a clearer view of the role of these amino acids within the active site and aid in the elucidation of the mechanism of AP endo.

[†] Supported by funds from the National Institutes of Health (Grant CA 72702 to P.R.S.) and Northeastern University and by grants from the National Institutes of Health (GM 40000, CA71993, and ES03926) to Bruce Demple.

[‡] A preliminary report of these findings has been published (*28*).

* To whom correspondence should be addressed.

[§] Northeastern University.

[||] Harvard School of Public Health.

[⊥] Current address: Department of Developmental Biology and Oncology, Research Institute for Radiation Biology and Medicine, Hiroshima University, Hiroshima, Japan.

[@] The Pennsylvania State University.

10.1021/bi982052v CCC: $18.00
Published on Web 04/01/1999

EXPERIMENTAL PROCEDURES

Site-Directed Mutagenesis. Three residues thought to be at the active site or directly involved in catalysis, Asp^{283}, Asp^{308}, and His^{309}, were selected for mutation (Figure 5). Four mutant proteins, D283A, D308A, D283A/D308A, and H309N, were prepared by site-directed mutagenesis (*9*), overexpression in BL21/DE3 *Escherichia coli* cells, and purification as described in ref *9*. In each case, the gene was sequenced to verify the mutation. Since all the mutants eluted in exactly the same position on each of the columns, gross misfolding during expression leading to loss of enzymatic activity was unlikely.

Enzyme Assays. Enzymatic assays were performed as described by Strauss et al. (*1*), using a substrate prepared from a double-stranded 45 bp oligomer containing a single G/U pair at position 21:

5'-AGC TAC CAT GCC TGC ACG AAU TAA GCA ATT CGT AAT CAT GGT CAT-3'
3'-TCG ATG GTA CGG ACG TGC TTG ATT CGT TAA GCA TTA GTA CCA GTA-5'

To generate the abasic site at position 21, single-stranded oligomer containing the uracil was labeled at the 5′-end and annealed with the complementary strand. This double-stranded oligomer was then treated with uracil DNA glycosylase (1 unit/100 pmol of U-containing oligonucleotide; Epicenter Technologies, Madison, WI) for 20−30 min at 37 °C in the presence of 0.1 M $NaBH_4$. Uracil DNA glycosylase was heat inactivated at 70−75 °C for 5 min. After cleavage with AP endo, the product was a 5′-^{32}P-labeled 20-mer with a hydroxyl group at the 3′-end and an unlabeled 24-mer with a phosphodeoxyribose at the 5′-end. The strand without the abasic site remained intact (*1*).

Steady state time course assays were carried out as described previously (*1*) in a 5 μL reaction volume at room temperature using 250 nM substrate over a 20−120 s time interval. The concentration of enzyme was 0.25−500 nM, depending on the mutant. The steady state concentration dependence was determined between 16 and 300 nM over a 20 s time interval for the D283A and the D308A mutants, a 30 s time interval for the D283A/D308A mutant, and a 180 s time interval for the H309N mutant. Enzyme concentrations are indicated in the legends of each figure. The incubation mixture for steady state assays contained 25 mM NaCl, 50 mM Hepes/NaOH (pH 7.5), 0.1 mM EDTA, and 5 mM $MgCl_2$. Since enzyme was diluted to 5 times the desired concentration in 50% glycerol in 50 mM Hepes, 1 mM EDTA, and 125 mM NaCl, the final concentration of Na^+ during the assay was 50 mM. The reaction was terminated by addition of EDTA to a final concentration of 87 mM. Substrate and product were resolved by gel electrophoresis by employing a 15% polyacrylamide gel in the presence of 8 M urea. The distribution of the isotope on the gel was determined by PhosphorImager analysis (Molecular Dynamics, Sunnyvale, CA).

Substrate binding under single-turnover conditions was assayed in a 5 μL reaction volume between 5 and 120 s using a range of substrate and enzyme concentrations (*1*). Binding by the wild type enzyme was performed with 0.4 nM enzyme and 4 nM substrate, while binding by the D283A or the D308A mutant was performed with 4 nM enzyme and 4 nM substrate. The effectiveness of the trap was demonstrated by achieving a constant E·S concentration, which occurred in the case of D308A by 40 s and in the case of D283A in <5 s. Attempts to measure the extent of binding by the D283A/D308A and the H309N mutants were performed with 4, 10, or 50 nM enzyme and 4, 10, or 80 nM substrate. Single-turnover assays were performed in 50 mM Hepes/NaOH (pH 7.5) containing 25 mM NaCl and 4 mM EDTA. As before, the enzyme dilution buffer contributed additional Na^+ to the final assay mix. The presence of EDTA prevented cleavage of substrate by the enzyme during the binding step and turnover. Enzymatic cleavage was initiated by the addition of 10 mM $MgCl_2$ in the presence of trap (2 mg/mL heparin and 6.1 μM HDP). The reaction was terminated 30 s later by the addition of EDTA to a final concentration of 87 mM. Kinetic simulation using the KINSIM kinetic simulation package (*10*) was used along with the data from the single-turnover experiments to approximate the forward (k_{on}) and backward (k_{off}) binding constants for the D283A and D308A mutants (Table 1).

Table 1: Comparison of Kinetic Constants of Wild Type AP Endo and AP Endo Mutants[a]

mutant	k_{cat} (s^{-1})	K_m (nM)	k_{cat}/K_m (M^{-1} s^{-1})	k_{on} (M^{-1} s^{-1})	k_{off} (s^{-1})	K_D (nM)
wild type	10	100	1×10^8	5×10^7	0.04	0.8
D283A	0.3	120	3×10^6	3×10^6	0.5	170
D308A	1.2	50	2×10^7	1×10^6	0.04	40
D283A/D308A	2×10^{-2}	240	8×10^4	ND	ND	−
H309N	3×10^{-4}	1300	2×10^2	ND	ND	−

[a] Constants calculated from data presented in Figures 3 and 4. K_D was obtained from the equilibrium concentration in single-turnover experiments (*18*). Substrate binding (k_{on}) and dissociation (k_{off}) rate constants were modeled by kinetic simulation. ND, not done.

Computer Simulations. For energy minimization analysis, we used starting coordinates of human AP endo provided P. Freemont (*4*). Mutant structures were created by replacing the appropriate residue(s) of the wild type crystal structure with the desired amino acid(s). All residues were represented using the AMBER all atom model (*11*). TIP3P (*12*) water molecules were added, where possible, at any point within 5.0 Å of each atom, using the EDIT module of AMBER 4.1 (*13*). Potential energy minimization calculations were then carried out for each mutant as well as for the wild type using ROAR 1.0 (*14*) with the standard 1994 AMBER force field (*15*). Each minimization was carried out for 2000 cycles. Minimized structures were then examined using Midas Plus (*16*) and Rasmol (*17*), and conformational shifts were measured.

RESULTS AND DISCUSSION

Steady State Measurements of AP Endo Mutant Activity Reveal Major Changes in Rate, but Minimal Changes in K_m. The time dependence for wild type AP endo and the four site-directed mutants was examined over a time interval of up to 180 s (Figures 1 and 2). Note that to demonstrate the time dependence of the nicking activity seen in Figure 1, different concentrations of enzyme were used. On the basis of initial rates of reaction at 250 nM substrate, both single aspartate mutants were 10−30-fold less active than the wild type while the double aspartate mutant was 500-fold less active and the histidine mutant was more than 30000-fold less active. The time course for nicking H309N was repeated at 10 nM enzyme and 250 nM substrate over intervals of up to 3 h with a similar result in the rate of nicking.

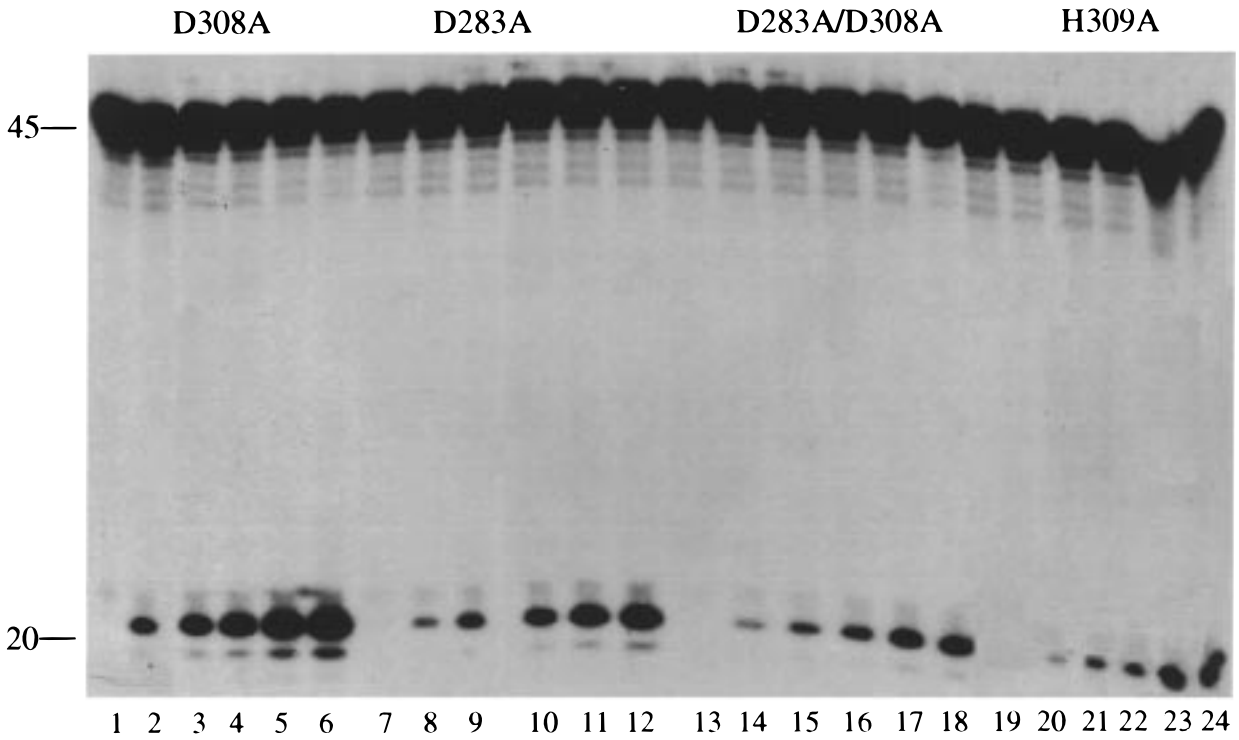

FIGURE 1: Time dependence of DNA nicking by AP endo mutants. The steady state time dependence of product formation by AP endo mutants was determined using 250 nM substrate. The reactions were initiated by the addition of either 1.0 nM D308A (lanes 1−7), 2.0 nM D283A (lanes 8−14), 20 nM D283A/D308A (lanes 15−21), or 500 nM H309N (lanes 22−28) and then terminated at 20, 40, 60, 120, and 180 s by the addition of EDTA. Substrate and product were resolved by gel electrophoresis employing a 15% polyacrylamide gel in the presence of 8 M urea.

The apparent K_m and k_{cat} values were examined for all four mutants and compared with that of the wild type enzyme (*1*). The apparent K_m values for D283A, D308A, D283A/D308A, and H309N were 120 nM ± 38% (SE), 50 nM ± 31% (SE), 240 nM ± 38% (SE), and 1300 nM ± 42% (SE), respectively. See Table 1. The k_{cat} values were 0.2 s^{-1} ± 14% (SE), 1.2 s^{-1} ± 9% (SE), 2×10^{-2} s^{-1} ± 21% (SE), and 3×10^{-4} s^{-1} ± 24% (SE), respectively. In contrast to the marked difference in catalytic activity shown by these rate studies, there was surprisingly little difference in the apparent K_m for the single and double aspartate mutants. The apparent K_m for the histidine mutant, however, was 13-fold higher than for the wild type (Figure 3 and Table 1). Hence, these studies support the likelihood that His^{309} is involved in catalysis. The enzymatic activity of the D283A mutant reported here is in sharp contrast to reports that this mutant had ~0.05% of the activity of the wild type (*7*). Since neither the substrate nor enzyme concentration was specified and since the substrate differed from the one used in these studies, it is difficult to make direct comparisons with the data presented here. However, the retention of substantial enzymatic activity on the part of D283A is consistent with the ability of this mutant to bind an abasic site-containing oligonucleotide as shown by other enzymatic and electrophoretic mobility shift assays (EMSA) (*9*).

Single-Turnover Measurements Show That D283A and D308A Bind Substrate in Different Manners. Substrate binding, determined using single-turnover conditions, was initiated by addition of enzyme to substrate in the presence of 4 mM EDTA to prevent nicking. The enzyme·substrate complex was then observed by activating nicking with Mg^{2+} in the presence of trap that prevented enzyme recycling. Binding and dissociation parameters were distinctly different for the wild type and the two single aspartate mutants (Figure 4). Binding curves for the double and histidine mutants could not be constructed despite repeated attempts over a range of concentrations of both substrate and enzyme due to the low stability of the enzyme·substrate complex. The equilibrium level of E·S for the wild type enzyme was 0.29 nM, measured at 0.4 nM enzyme and 4 nM substrate, conditions chosen because of the efficiency of binding by the wild type enzyme. The equilibrium level of E·S for the D283A mutant was 0.092 ± 0.009 nM (SE), measured at 4 nM enzyme and 4 nM substrate, while that for the D308A mutant was 0.32 ± 0.02 nM (SE), also measured at 4 nM enzyme and 4 nM substrate. (Note that the equilibrium level of binding for the wild type enzyme at the enzyme and substrate concentrations used with the mutant enzymes would have been 0.81 nM, as determined by kinetic simulation. This level is ~10 and 3 times greater than those of the D283A and D308A mutants, respectively.) Furthermore, the shapes of the binding curves for the wild type and for the two mutants were markedly different (Figure 4). The half-time for maximal binding for the wild type was ~5 s under the experimental conditions (data not shown and ref *1*); that for the D283A mutant was clearly <5 s, since maximal substrate was bound at the earliest measurement possible by this methodology, and that for the D308A mutant was 18−19 ± 4 s. The root-mean-square deviation of the calculated binding curve by D308A was ±0.35 fmol. In short, both equilibrium binding levels and $t_{1/2}$ values for the wild type and the mutants were different.

Kinetic Modeling Indicates That the Diminution of the Catalytic Efficiency by D283A and D308A Arises from

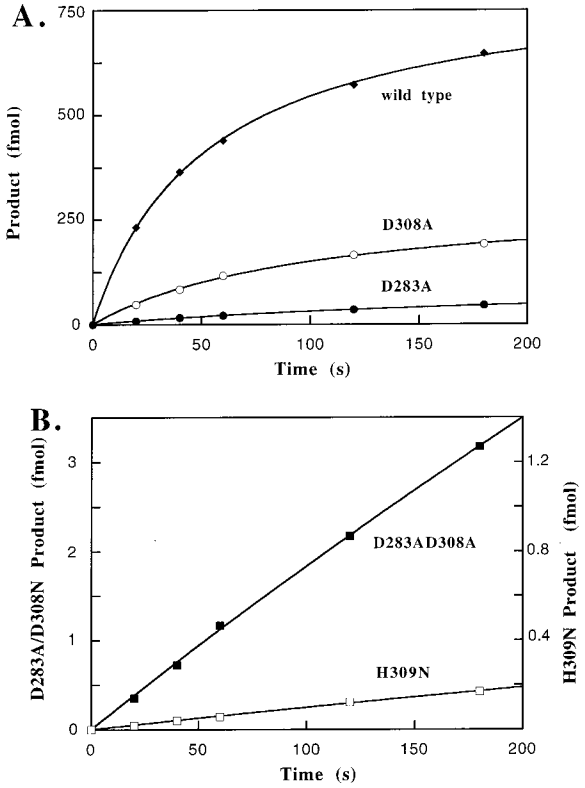

FIGURE 2: Quantitative analysis of the steady state time dependence for wild type AP endo and four site-directed mutants. Experimental data were obtained as described in Experimental Procedures and in the legend of Figure 1 and normalized to product formed per 0.25 nM enzyme. Data in this figure represent an average of two experiments for wild type AP endo (0.25 or 0.5 nM enzyme), five experiments each for D283A (2.0 nM enzyme) and D308A (1.0 nM enzyme), four experiments for D283A/D308A (20 or 50 nM enzyme), and three experiments for H309N (500 nM enzyme). (A) Comparison of wild type AP endo (◆), D283A (●), and D308A (○). The nicking rates (nanomoles of product per nanomole of enzyme per second) under these conditions were 10, 0.3, and 1.9 s^{-1} for wild type AP endo, D283A, and D308A, respectively. (B) Time course of D283A/D308A (■) and H309N (□). The nicking rates were 1.5×10^{-2} and 1.9×10^{-4} s^{-1}, respectively, under these conditions.

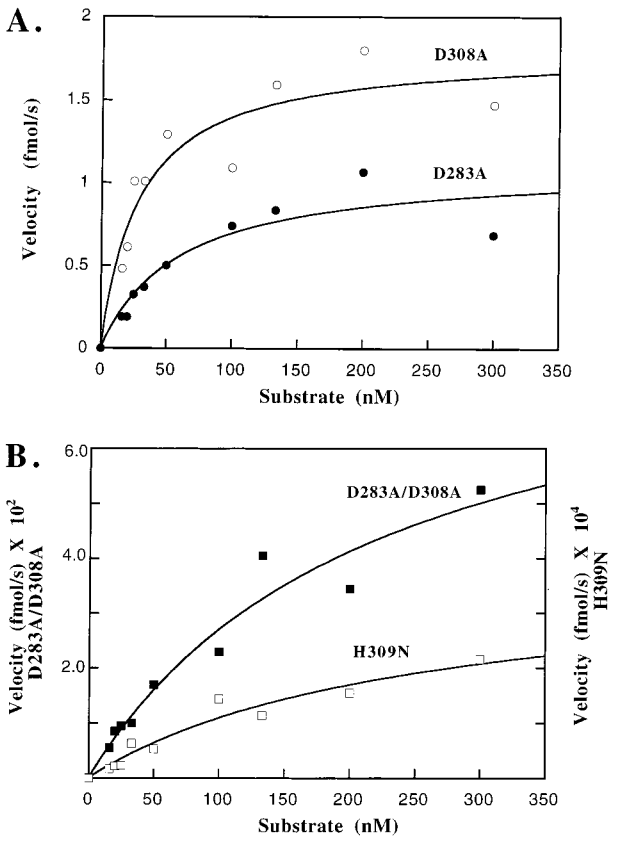

FIGURE 3: Steady state concentration dependence. Velocities are normalized to 1 nM enzyme, and data are based on an average of four experiments each for D283A and D308A and two experiments each for D283A/D308A and H309N. The k_{cat} and K_m values are shown in Table 1. (A) The concentration dependence for nicking by 1 nM D283A (●) and by 1 nM D308A (○) was determined between 16 and 300 nM over 20 s time intervals. (B) The concentration dependence was determined between 16 and 300 nM over 30 s time intervals for 50 nM D283A/D308A (■) and over 180 s time intervals for 500 nM H309N (□).

Different Sources. Kinetic simulation (*1*, *10*) allowed us to mimic the shape of the binding curves as well as the steady state levels of E·S to estimate binding and dissociation constants (Table 1). We showed previously that the wild type enzyme follows a Briggs−Haldane mechanism (Scheme 1)

Scheme 1

$$E + DNA_{abasic} \underset{k_{off}}{\overset{k_{on}}{\rightleftharpoons}} E^{DNA,abasic} \overset{k_2}{\rightleftharpoons} E^{DNA,nicked} \overset{k_3}{\rightleftharpoons} E + DNA_{nicked}$$

where K_m is approximated by $(k_{off} + k_2)/k_{on}$, k_2 is approximated by k_{cat}, and $k_3 \gg k_2$ (*18*). In Scheme 1, $E^{DNA,abasic}$ represents the enzyme·substrate complex and $E^{DNA,nicked}$ represents the enzyme·product complex. We considered k_2 to be a good approximation for k_{cat}, because we were unable to demonstrate a burst during the first turnover (*1*). The D283A mutant continued to follow the Briggs−Haldane scheme. However, for the D308A mutant the substrate association and dissociation rate constants (k_{on} and k_{off}, respectively) determined from the equilibrium levels of E·S and the shape of the binding curves (Figure 4) did not match the scheme shown above. Instead, the K_m was best approximated by the K_D, calculated as k_{off}/k_{on}. In general, as k_{cat} for an enzyme decreases and is no longer much greater than k_{off}, the K_m is best approximated by the K_D (*18*). However, since the k_{cat} obtained from steady state measurements was still 30 times *greater* than the k_{off} (see Table 1), while the K_m was *reduced* compared to that of the wild type, the simple Briggs−Haldane mechanism no longer applied to the D308A mutant.

The major difference between the single-turnover and the steady state experiments was the presence of 4 mM EDTA in the former studies during the step when enzyme bound to the abasic site-containing DNA. Since EDTA chelated remaining divalent cation, it prevented the enzyme from initiating catalysis and ensured that a true equilibrium was established between enzyme that was free of abasic site-containing DNA and enzyme that was bound to abasic site-containing DNA. Thereafter, catalysis was initiated by addition of divalent cation (Mg^{2+}) in the presence of trap, thereby limiting catalysis to a single round. One explanation for the failure to match the calculated K_m from Scheme 1 with the observed K_m could be that the D308A mutant kinetics revealed a step masked during steady state studies,

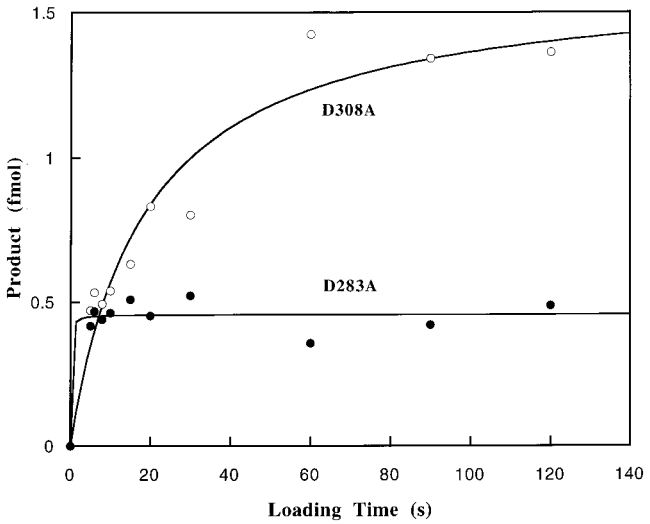

FIGURE 4: Single-turnover experiments. The extent of substrate binding to D283A (●) and D308A (○) was determined between 5 and 120 s. Substrate (4 nM) was allowed to bind to enzyme (4 nM) in the presence of 4 mM EDTA over the indicated time intervals, whereupon Mg^{2+} and trap were added to discharge the enzyme bound to an abasic site. Data are based on six experiments for D283A and five experiments for D308A. The forward (k_{on}) and backward (k_{off}) binding constants were calculated from the $t_{1/2}$ and the E·S concentration at equilibrium by kinetic simulation using the KINSIM kinetics simulation package (*10*). These values are reported in Table 1.

one that occurred so rapidly in the wild type and in the D283A mutant that it was transparent. Catalysis could only occur when the active site was properly aligned, which occurred when divalent cation was added to the reaction mixture. We exclude an effect occurring after catalysis because such a post catalytic event would not have resulted in alteration of the rate of binding and dissociation and the *decreased* K_m. We propose that, when divalent cation was absent, the conversion of Asp^{308} to alanine might alter the conformation of the enzyme in such a way that not only was catalysis disabled but also the enzyme had to undergo a realignment. Ordinarily, any realignment that might be necessary occurred so quickly that it did not appear in the kinetic scheme. However, when alanine was substituted for Asp^{308}, alignment proceeded so slowly that it was necessary to insert it into the kinetic scheme as depicted in Scheme 2 below:

Scheme 2

(A) binding assay

$$E + DNA_{abasic} \underset{k_{off(EDTA)}}{\overset{k_{on(EDTA)}}{\rightleftharpoons}} E^{DNA,abasic} \overset{Mg^{2+}}{\rightleftharpoons}$$

$$E(Mg^{2+})^{DNA,abasic} \overset{k_{cat}}{\rightleftharpoons} E(Mg^{2+})^{DNA,nicked} \overset{k_{diss}}{\rightleftharpoons} E(Mg^{2+}) + DNA_{nicked}$$

(B) steady state

$$E(Mg^{2+}) + DNA_{abasic} \underset{k_{off}}{\overset{k_{on}}{\rightleftharpoons}} E(Mg^{2+})^{DNA,abasic} \overset{k_{cat}}{\rightleftharpoons}$$

$$E(Mg^{2+})^{DNA,nicked} \overset{k_{diss}}{\rightleftharpoons} E(Mg^{2+}) + DNA_{nicked}$$

Thus, the conversion of $E^{DNA,abasic}$ to $E(Mg^{2+})^{DNA,abasic}$ would involve a conformational change that became partially rate-limiting for the D308A mutant. At this time, we feel it is unlikely that the enzyme ordinarily dissociates from Mg^{2+} with each catalytic round. In that case, the sequence of steps would always involve the conformational change proposed for the D308A mutant as well as a final step where enzyme and divalent cation dissociate from one another. Then the dissociation and reassociation steps would appear in the steady state kinetics for D308A, which they do not. In other studies using rapid start EMSA, the response to Mg^{2+} was also complex with effects on both stability of the E·S complex and dissociation of product (*19*). Furthermore, the response of the D308A mutant differed from those of both the wild type and D283A mutant.

Molecular Modeling Analysis Suggests That Multiple Residues Shift Position When either Asp^{283} or Asp^{308} Is Mutated. Changes in primary structure of a protein are often accompanied by unexpected perturbations in local tertiary structure. Although such minimization methods are theoretical algorithms and are subject to error, there is a remarkable concordance where minimizations performed with ROAR in an AMBER force field have been compared with solved crystal structures (*20*). To examine possible changes in configuration at the active site of AP endo upon site-directed mutagenesis, we performed molecular minimization analysis using ROAR in an AMBER force field on mutations mapped onto AP endo. The locations of residues with major shifts relative to the minimized wild type (>0.5 Å) are illustrated in Figure 5. In particular, mutation of Asp^{283} to alanine resulted in displacing of Ser^{66} by 1.8 Å and of Cys^{310} by 2.06 Å and in tilting of the entire His^{309} side chain by ~0.5 Å. Despite the fact that Asp^{283} hydrogen bonds with Thr^{265} in the crystal structure as noted by Gorman et al. (*4*), Thr^{265} was not disturbed by the replacement of this aspartate with alanine. Both Ser^{66} and Cys^{310} are highly conserved residues (*4*), making it even more likely that they play roles in enzymatic activity. Although the shift in Cys^{310} occurred with both aspartate mutations (see below), the shift in Ser^{66} was unique to the D283A mutant. Since Ser^{66} is not within hydrogen bonding distance of any residue in the wild type or mutant enzymes, it would be free to hydrogen bond with water or an incoming nitrogen of a DNA base. Consequently, we propose that Ser^{66} may interact directly with either substrate, product, or both. In short, the D283A mutation disturbed binding of substrate to the active site but not the ability of the enzyme to rapidly adopt the conformation necessary to perform the catalytic step. Furthermore, while Asp^{283} is clearly important in maintaining the alignment of His^{309}, it is not directly involved in catalysis as has been proposed previously (*5*, *6*). Neither Ser^{66} nor Cys^{310} has been noted in previous mutagenesis studies with AP endo (*5*−*9*).

In contrast to the changes that were predicted to occur in the D283A mutant, the predicted changes in tertiary structure for the D308A mutant involved many more residues and the disruption extended over a greater distance. While active site His^{309} remained unchanged relative to the wild type, numerous residues in the vicinity of His^{309} shifted position. Of particular note were Thr^{97}, which shifted by 1.24 Å; Lys^{98}, where the entire side chain shifted by ~1.3 Å; Trp^{267}, which shifted by 0.97 Å; Thr^{268}, where the entire side chain shifted by 2.06 Å; Tyr^{269}, where the entire side chain shifted out of the plane by 1.3 Å; Arg^{274}, where the side chain shifted by 0.94 Å; Asn^{212}, which shifted by 1.17 Å; Cys^{310}, which

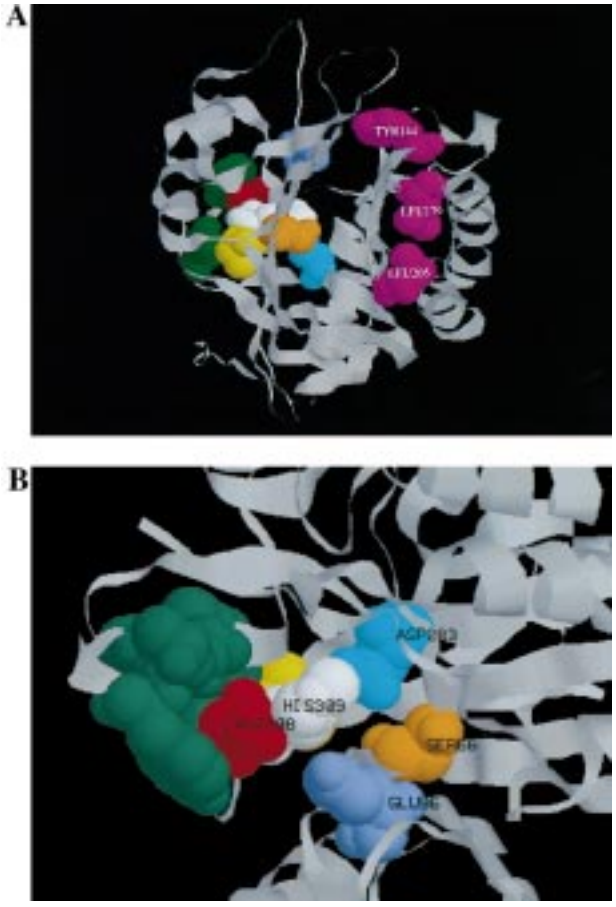

FIGURE 5: (A) Three-dimensional structure of AP endo, showing the residues mutated in this study and the residues likely to be affected by the mutations, as determined from molecular modeling: white, His^{309}; red, Asp^{308}; cyan, Asp^{283}; yellow, Cys^{310}; light blue, Glu^{96}; orange, Ser^{66}; and green, Tyr^{269}, Arg^{274}, Thr^{268}, Trp^{267}, Thr^{97}, Lys^{98}, and Asn^{212}. Also shown in magenta are Tyr^{144}, Leu^{179}, and Leu^{205}, the three residues in contact with substrate or product identified by domain mapping experiments (*24*). (B) Enlargement of the active site region shown in panel A.

shifted by 2.29 Å; and, finally, Glu^{96}, where the entire side chain shifted by ~1.4 Å. The shift in Cys^{310} is the only alteration to occur in both aspartate single mutants. Many of the disrupted residues are highly conserved, including Glu^{96}, Thr^{97}, Lys^{98}, Asn^{212}, Tyr^{269}, and Trp^{267} (*4*, *8*). Of these residues, replacement of Asn^{212} with alanine, aspartic acid, or glutamine greatly diminished the ability to cleave an abasic site or retard the movement of an oligonucleotide containing an abasic site during electrophoresis on a nondenaturing gel (*7*). Indeed, the shift in Glu^{96} is noteworthy in that it did *not* occur in the D283A mutant. Glu^{96} along with Asp^{308} has been proposed to play a key role in positioning the Mg^{2+} at the active site (*4*−*6*, *8*). If Asp^{308} were the critical residue for binding to the divalent cation, then the D308A mutant should be devoid of enzymatic activity, which it is not. If, on the other hand, Asp^{308} along with other residues that shift in its absence serves instead to position Glu^{96}, then replacement of Asp^{308} with alanine would result in the observed effects. Indeed, assay in the presence of Ca^{2+} instead of Mg^{2+} restores the full enzymatic activity of D308A (data not shown). Since the larger divalent cation restores catalytic function, it probably offsets the displacement of Glu^{96}, providing support for the argument that displacement of Glu^{96} determined the observed kinetic effects. Also, we note that similar molecular modeling of exonuclease III with the mutation equivalent to D308A resulted in a large displacement in the equivalent glutamate residue. In sum, despite multiple predicted shifts of as much as 2.29 Å in the D308A mutant, the k_{cat} dropped by only 1 order of magnitude and the k_{on} decreased 50-fold. However, the ability of the mutant to recover the tertiary structure necessary for catalysis was diminished substantially to the point where a conformational shift involved with binding Mg^{2+} became a part of the catalytic scheme.

The predicted changes in conformation of the double aspartate mutant by molecular modeling were roughly equivalent to the sum of the changes in the individual mutants. The observed kinetic changes involved a 500-fold decrease in the k_{cat} and a 125-fold decrease in the catalytic efficiency. The extent of substrate binding could not be measured in single-turnover experiments. Furthermore, changes in the Arrhenius activation were calculated for the wild type enzyme, the single aspartate mutants, and the double aspartate mutant. The $\Delta\Delta G°$ for the double mutant relative to the wild type enzyme[1] was 15.2 kJ, which is approximately the sum of the difference of the two single mutants ($\Delta\Delta G° = 8.6$ kJ for the D283A mutant and $\Delta\Delta G° = 5.2$ kJ for the D308A mutant). On this basis, both aspartate residues were probably involved independently in maintaining the proper conformation of the active site so as to enable efficient catalysis.

Kinetic Measurements Combined with Molecular Minimization Analysis of AP Endo Mutants Provide Insight into the Molecular Mechanism of Abasic Site Nicking. Two major models for cleavage by AP endo have been proposed. The first is based on similarities of the nuclease fold in DNase I (*21*), exonuclease III (*22*), and AP endo (*5*) and the fact that DNase I has been cocrystallized with DNA (*21*). The active site of the enzyme is postulated to lie in a pocket at the top of the $\alpha\beta$ sandwich and is surrounded by loop regions. One of these loops involves α-helix 5. The attacking nucleophile is a hydroxide ion obtained through deprotonation of water by His^{309}. The single divalent cation aids in the attack on the labile phosphate by either polarizing the P−O3′ bond (*8*) or stabilizing it (*4*).The second model argues that the nucleophile that attacks the C3′ of the deoxyribose located 5′ to the abasic site is one of the ring nitrogens of His^{309} itself rather than an activated water and that the divalent cation serves to orient His^{309} and stabilize its electronic distribution. Neither model takes into account the possibility that the enzyme changes conformation when it binds substrate or product or that substrate and product may bind differently to the enzyme whether or not it changes conformation. Since there are currently no X-ray crystallographic data for a cocrystal of DNA containing an abasic site with either AP endo or exonuclease III, it is not possible to decide which model is correct. Furthermore, despite clear evidence from NMR studies that the structure of DNA in the neighborhood of an abasic site depends on the sequence context (*23*, *24*), AP endo appears to have no sequence

[1] ΔG for the wild type enzyme was calculated according to transition state theory (*18*) as $RT \ln(k_{cat}/K_m \times h/kT) = -\Delta G^{‡} - \Delta G_S$, where k is the Boltzmann constant and h is Planck's constant. ΔG_S was obtained from the single-turnover equilibrium binding level as $\Delta G_S = -RT \ln K_e$. The changes in Arrhenius activation energy relative to the wild type enzyme were calculated as $\ln(k_{cat,wildtype}/k_{cat,mutant}) = (-E_{a,wildtype} + E_{a,mutant})/RT$.

preference (*25*; D. Carey and P. Strauss, manuscript in preparation). Hence, NMR studies with abasic site-containing DNA by itself may provide insight about structural changes in DNA containing an abasic site but are probably not so helpful in predicting how the enzyme interacts with its substrate. Finally, on the basis of copper phenanthroline footprinting, abasic site-containing DNA undergoes a structural distortion in binding to the enzyme (*26*), and on the basis of domain mapping by limited proteolysis (*27*), it is likely that substrate containing an abasic site and product containing the nicked abasic site bind differently to the enzyme.

Thus, the data presented in this study clearly support a role for two active site aspartates, Asp^{283} and Asp^{308}, that spatially flank the catalytically active His^{309}. Each plays a distinct role in maintaining the integrity of the active site, the orientation of His^{309}, and the supporting residues such as Glu^{96} and Ser^{66}. They also support a role for Asp^{308} in maintaining the orientation of Glu^{96}, which may bind the catalytically critical divalent cation.

ACKNOWLEDGMENT

We are grateful to Dr. Kenneth Merz for making the ROAR program with standard 1994 AMBER force field available for this work, to Dr. Paul Freemont for providing the coordinates of human AP endonuclease before deposition in the Brookhaven Protein Data Bank, and to Dr. William Beard for helpful discussions on interpretations of kinetic data.

REFERENCES

1. Strauss, P. R., Beard, W. A., Patterson, T. A., and Wilson, S. H. (1997) *J. Biol. Chem. 272*, 1302−1307.
2. Doetsch, P. W., and Cunningham, R. P. (1990) *Mutat. Res. 236*, 173−201.
3. Demple, B., and Harrison, L. (1994) *Annu. Rev. Biochem. 63*, 915−948.
4. Gorman, M. A., Morera, S., Rothwell, D. G., de La Fortelle, E., Mol, C. D., Tainer, J. A., Hickson, I. D., and Freemont, P. S. (1997) *EMBO J. 16*, 6548−6558.
5. Barzilay, G., and Hickson, I. D. (1995) *BioEssays 17*, 713−719.
6. Barzilay, G., Walker, L. J., Robson, C. N., and Hickson, I. D. (1995) *Nucleic Acids Res. 23*, 1544−1550.
7. Rothwell, D. G., and Hickson, I. D. (1996) *Nucleic Acids Res. 24*, 4217−4221.
8. Barzilay, G., Mol, C. D., Robson, C. N., Walker, L. J., Cunningham, R. P., Tainer, J. A., and Hickson, I. D. (1995) *Nat. Struct. Biol. 2*, 561−568.
9. Masuda, Y., Bennett, R. A. O., and Demple, B. (1998) *J. Biol. Chem. 273*, 30352−30359.
10. Wachsstock, D. H., and Pollard, T. D. (1994) *Biophys. J. 67*, 1260−1273.
11. Weiner, S. J., Kollman, P. A., Case, D. A., Singh, U. C., Ghio, C., Alagona, G., Profeta, S., and Weiner, P. (1984) *J. Am. Chem. Soc. 106*, 765−784.
12. Jorgensen, W. L., Chandrasekhar, J., Madura, J. D., Impey, R. W., and Klein, M. L. (1983) *J. Chem. Phys. 79*, 926−935.
13. Pearlman, D. A., Case, D. A., Caldwell, J. C., Seibel, G. L., Singh, U. C., Weiner, P., and Kollman, P. A. (1991) *AMBER*, version 4.1, The University of California, San Francisco.
14. Cheng, A., Stanton, R. S., Vincent, J. J., Damodaran, K. V., Dixon, S. L., Hartsough, D. S., Mori, M., Best, S. A., and Merz, K. M., Jr. (1997) *ROAR*, version 1.0, The Pennsylvania State University, University Park, PA.
15. Cornell, W. D., Cieplak, P., Bayly, C. I., Gould, I. R., Merz, K. M., Jr., Ferguson, D. M., Spellmeyer, D. C., Fox, T., Caldwell, J. W., and Kollman, P. A. (1995) *J. Am. Chem. Soc. 117*, 5179−5197.
16. Ferrin, T. E., Huang, C. C., Jarvis, L. E., and Langridge, R. (1988) *J. Mol. Graphics 6*, 2−12.
17. Sayle, R. A., and Milner-White, E. J. (1995) *Trends Biochem. Sci. 20*, 374−379.
18. Fersht, A. (1985) *Enzyme Structure and Mechanism*, 2nd ed., W. H. Freeman and Co., New York.
19. Masuda, Y., Bennett, R. A. O., and Demple, B. (1998) *J. Biol. Chem. 273*, 30360−30365.
20. Kini, R. M., and Evans, H. J. (1991) *J. Biomol. Struct. Dyn. 9*, 475−488.
21. Suck, D., and Oefner, C. (1986) *Nature 321*, 620−625.
22. Mol, C. D., Kuo, C.-F., Thayer, M. M., Cunningham, R. P., and Tainer, J. A. (1995) *Nature 374*, 381−386.
23. Gelfand, C. A., Plum, G. E., Grollman, A. P., Johnson, F., and Breslauer, K. J. (1996) *Biopolymers 38*, 439−445.
24. Beger, R. D., and Bolton, P. H. (1998) *J. Biol. Chem. 273*, 15565−15573.
25. Wilson, D. M., III, Takeshita, M., Grollman, A. P., and Demple, B. (1995) *J. Biol. Chem. 270*, 16002−16007.
26. Wilson, D. M., III, Takeshita, M., and Demple, B. (1997) *Nucleic Acids Res. 25*, 933−939.
27. Strauss, P. R., and Holt, C. M. (1998) *J. Biol. Chem. 273*, 14435−14441.
28. Lucas, J. A., Masuda, Y., Bennett, R. A. O., and Strauss, P. R. (1997) *FASEB J. 11*, A1192.

BI982052V